The Essential Dynamics of Cu, Zn Superoxide Dismutase: Suggestion of Intersubunit Communication

G. Chillemi,*# M. Falconi,§ A. Amadei,¶ G. Zimatore,*|| A. Desideri,§ and A. Di Nola*

*Department of Chemistry, University of Rome "La Sapienza," 00185 Rome, Italy; #Consorzio per le Applicazioni di Supercalcolo per Università e Ricerca, c/o Università "La Sapienza," 00185 Rome, Italy; §Istituto Nazionale Fiscia Della Materia and Department of Biology, University of Rome "Tor Vergata," 00173 Rome, Italy; ¶Reseach Institute and Laboratory of Biophysical Chemistry, University of Groningen, 9747 AG Groningen, The Netherlands; and ||Istituto di Strutturistica Chimica, Consiglio Nazionale Delle Ricerche Montelibretti, Rome, Italy

ABSTRACT A 300-ps molecular dynamics simulation of the whole Cu, Zn superoxide dismutase dimer has been carried out in water, and the trajectory has been analyzed by the essential dynamics method. The results indicate that the motion is defined by few preferred directions identified by the first four to six eigenvectors and that the motion of the two monomers at each instant is not symmetrical. The vectors symmetrical to the eigenvectors are significantly sampled, suggesting that, on average, the motions of the two subunits will exchange. Large intra- and intersubunit motions involving different subdomains of the protein are observed. A mechanical coupling between the two subunits is also suggested, because displacements of the loops surrounding the active site in one monomer are correlated with the motion of parts of the second toward the intersubunit interface.

INTRODUCTION

Cu, Zn superoxide dismutases (SODs; EC 1.15.1.1) are ubiquitous metalloenzymes that catalyze the dismutation of superoxide into oxygen and hydrogen peroxide by alternating reduction and oxidation of a copper ion that constitutes the active redox center (Bannister et al., 1987). The structure-function relationship of Cu, Zn SODs is now quite well understood from solution studies of native and site-directed mutated enzymes (Getzoff et al., 1992; Fisher et al., 1994; Polticelli et al., 1995, 1996) and from the available three-dimensional structures (Tainer et al., 1982; Djinovich et al., 1992; Djinovich-Carugo et al., 1996). The diffusion of the negatively charged substrate may be modulated by the distribution of the electrostatic potential around the protein (Klapper et al., 1986; Sines et al., 1990), which has been suggested to be constant in the evolution of this enzyme (Desideri et al., 1992; Sergi et al., 1994).

The folding of the amino acid polymer is globular and is constituted by two identical subunits of 16 kDa, which have been called Orange and Yellow, respectively (Tainer et al., 1982). Each subunit is composed of a flattened cylinder (called a β-barrel) and three major external loops, which form almost half of the subunit (Tainer et al., 1982) (Fig. 1). The β-barrel structure is constituted by two β-sheets; one is composed of four regular (1–4) and the other by four twisted (5–8) β-strands joined by three large loops (6, 5–7, 8, and 4, 7) and by four turns. In combination with loops 6,5 and 7,8, the latter, less regular β-sheet, accommodates the active site. Loop 4,7 joins β-strands belonging to different sheets, and the other two large loops (loops 6, 5 and 7, 8) form a deep crevice connecting the solvent and the external surface of the barrel. The copper and zinc atoms are located at the bottom of this channel and are coupled together by a bridging imidazolate side chain (His61). The Zn^{2+} ion is coordinated by two more histidyl residues and one aspartyl residue (His69, His78, Asp81). The catalytically active Cu^{2+} ion is accessible to the solvent and is coordinated by three additional histidyl residues (His44, His46, His118) and by one water molecule (Tainer et al., 1982), which is in fast exchange with the bulk water (Gaber et al., 1972) and which may be substituted by the incoming anion inhibitors or substrate (Getzoff et al., 1983; Djinovich-Carugo et al., 1994).

Some dynamical properties of this protein have been investigated by experimental and theoretical approaches. The protein average dynamics, worked out through a quasi-elastic neutron scattering study (Andreani et al., 1995), indicated a mean square displacement of the nonexchangeable protons comparable to that observed in myoglobin (Doster et al., 1989). Analysis of the electronic absorption spectra of the metals as a function of temperature indicated a dynamical coupling with the solvent for the copper but not for the zinc site (Cupane et al., 1994, 1995). Molecular dynamics (MD) simulations of the bovine protein (Shen et al., 1989; Shen and McCammon, 1991; Y. Wong et al., 1993) and homology models of native and mutant human Cu, Zn SOD (Banci et al., 1992, 1994) pointed out the importance of the mobility of the active site channel for interaction with the substrate. All of these MD studies have been performed on a simulation system composed of one monomer and part of the second, including the interface region. Recently a 100-ps MD simulation (Falconi et al., 1996) on the whole dimer suggested the occurrence of two

Received for publication 17 January 1997 and in final form 8 May 1997.

Address reprint requests to Dr. Alessandro Desideri, Department of Biology, University of Rome "Tor Vergata," Via della Ricerca Scientifica, 00133 Rome, Italy. Tel.: +39-6-72594376; Fax: +39-6-72594311; E-mail: desideri@utovrm.it.

0006-3495/97/08/1007/12 $2.00

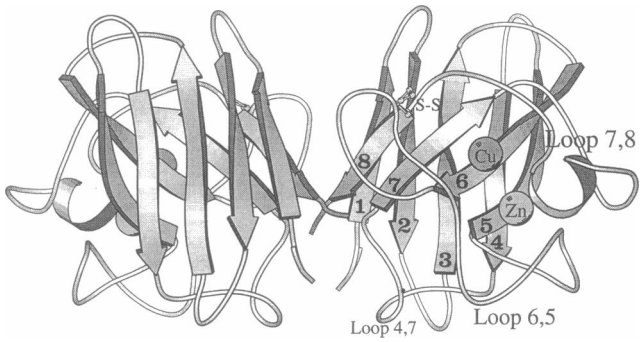

FIGURE 1 Schematic view of the bovine Cu, Zn superoxide dismutase dimer. The arrows indicate the β-strands (β-strands 1–4 form the regular β-sheet, whereas β-strands 5–8 form the irregular β-sheet). The three major loops and the four turns are represented as thin wires. The disulfide bridge (S-S) is indicated by the ball-and-stick representation. The spheres represent the metal ions. The picture was produced with the MolScript v1.4 program (Kraulis, 1991).

different conformational substates for the two monomers. To better understand such a phenomenon, we decided to carry out an essential dynamics analysis on this enzyme.

Essential dynamics has been shown to be a very useful tool for finding evidence of the protein regions where the motion is mainly localized, and since its introduction (Amadei et al., 1993) it has been successfully applied to describing the dynamical characteristics of several monomeric proteins (Amadei et al., 1993; van Aalten et al., 1995; Scheek et al., 1995).

In this study we report for the first time the essential dynamics analysis of a 300-ps MD simulation of a whole dimeric molecule in water to investigate and highlight the principal motions due to the protein dimericity. The results indicate an instantaneous asymmetrical dynamical behavior of the two monomers, the confinement of the largest displacements in the region constituted by the active site loops, and the presence of correlated motions that suggest the occurrence of a mechanical coupling between the two subunits.

METHODS

Molecular dynamics simulation has been performed with the parallel version of GROMOS (van Gunsteren and Berendsen, 1987) realized under the EUROPORT2 program (Parallelization for Computational Chemistry PACC consortium) of the European Commission. Calculations have been carried out on a Silicon Graphics Power Challenge (16 nodes shared memory) platform.

The coordinates of the Orange/Yellow Cu, Zn SOD dimer at 2-Å resolution (Tainer et al., 1982) were obtained from the Brookhaven Protein Data Bank (Bernstein et al., 1977). The dimeric molecule was immersed in a rectangular box of dimensions $61 \times 65 \times 82$ Å^3, filled with 9436 water molecules. For the active site metal cluster, ab initio calculated atomic partial charges were used (Shen et al., 1990). Nonpolar hydrogen atoms were not included in the calculation, and the united atom approach was applied. The protein, including polar hydrogen atoms, contained 2678 atoms. A total of 158,000 steps of 2 fs were performed, reaching a total simulation time of 316 ps. The CPU time for the simulation of each step was 2.2 s.

The protocol for the equilibration was the following:

1. Ten picoseconds of solvent equilibration with the protein atoms fixed
2. Ten-picosecond simulation of the whole system, starting at a temperature of 10 K and ending at a temperature of 298 K
3. Simulation (316 ps) at $T = 298$ K.

The first 50 ps of the simulation was used for equilibration, and the remaining 266 ps was used for analysis. The temperature was kept constant at 298 K by coupling the system to an external bath (Berendsen et al., 1984). Bond lengths were constrained by the SHAKE procedure (Ryckaert et al., 1977), and nonbonded interactions were evaluated using a cutoff of 8.0 Å. Protein and solvent configurations were saved every 50 steps, so that 3160 frames were stored. The trajectory was checked to assess the quality of the simulation, and the essential degrees of freedom were extracted according to the method developed by Amadei (Amadei et al., 1993) by using the program WHATIF (Vriend, 1990). The method, equivalent to a principal component analysis on the coordinate fluctuations (Garcia, 1992; Romo et al., 1995) and related to quasi-harmonic analysis (Ichiye and Karplus, 1991; Hayward et al., 1993), allows separation of the configurational space into subspaces: an essential subspace, in which most of the positional fluctuations can be described by a few coordinates, and a remaining subspace including all of the coordinates with an approximate constrained harmonic character. The essential dynamics method is based on the construction of the correlation matrix of the coordinate fluctuations:

$$\tilde{C} = \mathrm{cov}(x) = \langle (x - \langle x \rangle)(x - \langle x \rangle)^{\mathrm{T}} \rangle \qquad (1)$$

After removal of the translational and rotational degrees of freedom, the matrix $\tilde{C}$ was built up and then diagonalized to obtain the eigenvectors and eigenvalues, which give information about correlated motions throughout the protein. By ordering the eigenvectors, according to decreasing value of the eigenvalues, the most relevant eigenvectors can be detected. In the present case, because of the large size of the macromolecule investigated, the correlation matrix was built up only for the protein C_α atoms. It has already been shown that this choice gives a correct picture of the essential subspace (Amadei et al., 1993).

RESULTS

Structural check

Geometrical properties of Cu, Zn superoxide dismutase were monitored during the whole trajectory as a measure of

structural stability. This check was done iteratively with the DSSP program (Kabsch and Sander, 1983), using the molecular dynamics frames as input and by comparing them with the minimized x-ray structure.

To control the structural stability of the protein, the following geometrical properties have been monitored: the total accessible surface area of the protein dimer, the number of residues in unfavorable regions of the Ramachandran plot, the number of residues in random coil conformation, the number of backbone hydrogen bonds, the gyration radius for the C_α structures, the percentages of secondary structure, and the r.m.s.d. from the minimized x-ray structure in each SOD monomer. The time dependences of these variables are reported in Fig. 2 and 3. For the sake of clarity, both the averages and the root mean square fluctuations (r.m.s.f.) are reported in Table 1, in comparison with the corresponding values observed in the minimized crystal structure. Fig. 2 shows that the largest variation in the parameters, with respect to the crystallographic structure, occurred within the first 50 ps. The structural parameters b, c, d, and e in Fig. 2 do not change appreciably during the remaining simulation, whereas the total accessible surface

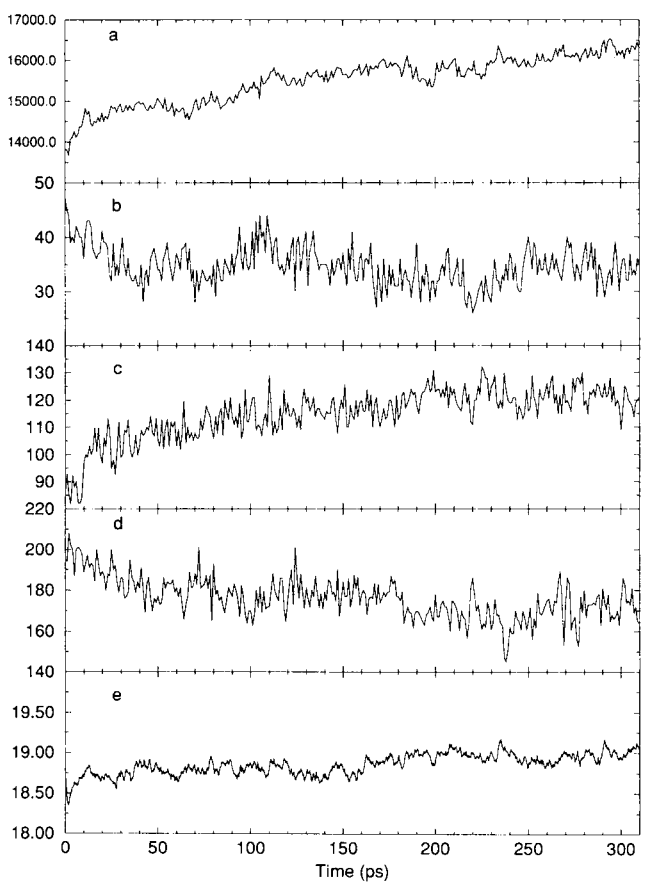

FIGURE 2 Time dependence of SOD geometrical properties. (*a*) Total accessible surface area of the protein dimer (Å^2). (*b*) Number of residues in unfavorable regions of the Ramachandran plot. (*c*) Number of residues in random coil conformation. (*d*) Number of backbone's hydrogen bonds. (*e*) Gyration radius for the C_α structures (Å).

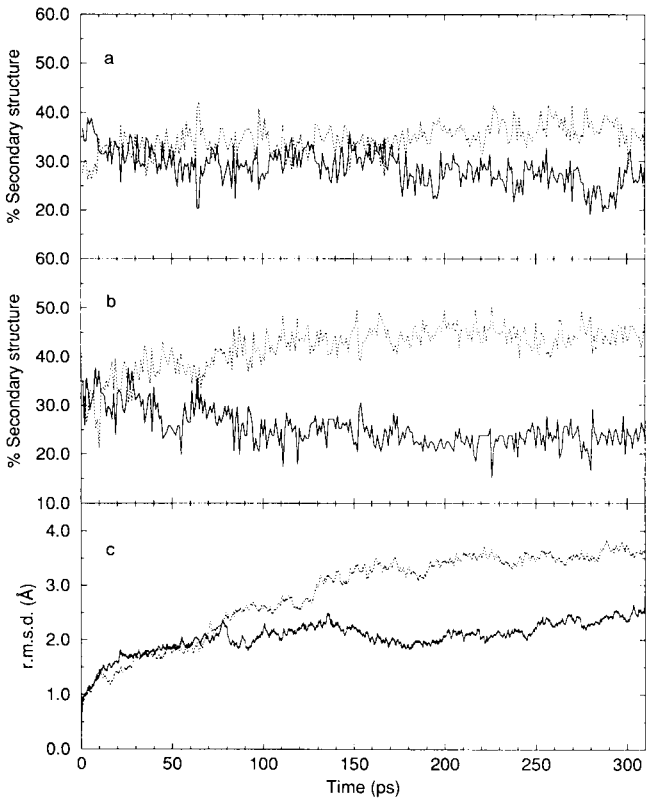

FIGURE 3 Time dependence of the percentage of β (——) and random-coil (·····) structure in the orange (*a*) and yellow (*b*) SOD monomers. (*c*) Time course of the all-atom r.m.s. deviation from the minimized x-ray structure of the orange (——) and the yellow (·····) subunits.

area of the dimer reaches a constant value in the second half of the simulation. The increase in the total accessible surface area and the constancy of the other parameters indicate that the protein maintains its structure and that the fluctuations are mainly localized on the loops.

The percentage of secondary structure, calculated for each subunit shown in Fig. 3, is indicative of asymmetrical motion in the two monomers. In the Orange subunit the percentage does not change during the trajectory. In the Yellow subunit the percentage of the β structure is reduced slightly, and there is a corresponding increase in the random coil. It has been shown that the β-sheet structure can easily be deformed during dynamics simulations (Sneddon and Brooks, 1993). Sheets can undergo backbone dihedral oscillations without losing hydrogen bond energy due to the curvature of the $\phi - \psi$ potential energy surface that is smaller in the β-region than in the α-region. In the case of SOD, this alteration does not perturb the correct globular folding, as confirmed by the total number of main-chain hydrogen bonds that is maintained in the whole dimer (see Table 1). The asymmetry of the two monomers is also confirmed by the time course of the all-atom r.m.s.d. from the minimized x-ray structure of the two separate subunits (Fig. 3 *c*).

The exchange of water molecules in the active site has been analyzed for each subunit as a function of time. In the

TABLE 1 Geometrical properties and fluctuations

Geometrical property	Reference	MD average	r.m.s.f.
Total solvent accessible surface area of the dimer (Å^2)	13755	15525	581
Residues outside the allowed Ramachandran regions	49.0	34.7	3.6
Residues in random coil conformation	95	115	9
Main-chain to main-chain hydrogen bonds	188	176	10
Gyration radius of C_α atoms (Å)	19.6	18.9	0.1
% of β structure in Orange subunit	35.10	28.78	3.56
% of random coil structure in Orange subunit	28.48	34.62	2.91
% of β structure in Yellow subunit	28.00	25.22	3.79
% of random coil structure in Yellow subunit	34.67	42.01	4.46

Yellow subunit, one water molecule remains close to the copper (average Cu-O distance 3.0 Å), whereas in the Orange subunit four water molecules (average Cu-O distance 2.9 Å) exchange with the bulk and alternately approach the copper atom.

Essential dynamics analysis

Fig. 4 shows a plot of the eigenvector index against eigenvalues, derived from the covariance matrix obtained from the solvent simulation trajectory.

There are only a few eigenvectors with large eigenvalues, as already reported for lysozyme (Amadei et al., 1993), thermolysin (van Aalten and Amadei, 1995), and HPr (Scheek et al., 1995), showing that the protein motion occurs mainly along very few directions in the essential subspace. The fractional contribution to the overall motion appears as an inset in the figure.

The components of the first four eigenvectors are reported in Fig. 5 for each monomer. From the figure it is evident that the amplitude of the essential motions of the two monomers is different, indicating the occurrence of an instantaneous asymmetry. In particular, in the first two eigenvectors, a larger motion is observed in the Yellow monomer than in the Orange one. The opposite occurs for eigenvectors 3 and 4, in which the Yellow monomer is less mobile than the Orange one. It is also interesting to note that in both monomers the largest displacements occur in the residues belonging to the electrostatic loop 7,8, which is involved in the substrate steering toward the catalytic copper (Klapper et al., 1986; Sines et al., 1990). It can be noted that each eigenvector has components of nonnegligible intensity in both subunits. This is particularly evident for loops 7,8 and 6,5. This is evidence of a correlation between the subunits and suggests the presence of a mechanical coupling between them. In Fig. 6 the projections of the C_α

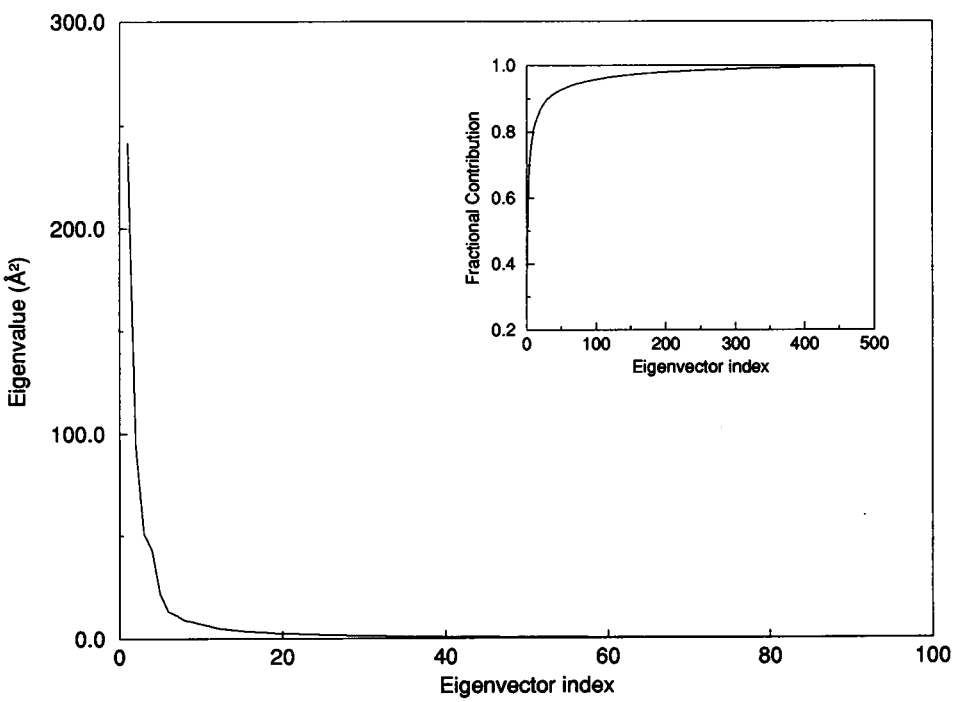

FIGURE 4 Plot of eigenvalues against corresponding eigenvector indices derived from the covariance matrix constructed from the simulation. The eigenvectors are sorted by decreasing eigenvalue. (*Inset*) Fractional contribution to the overall motion.

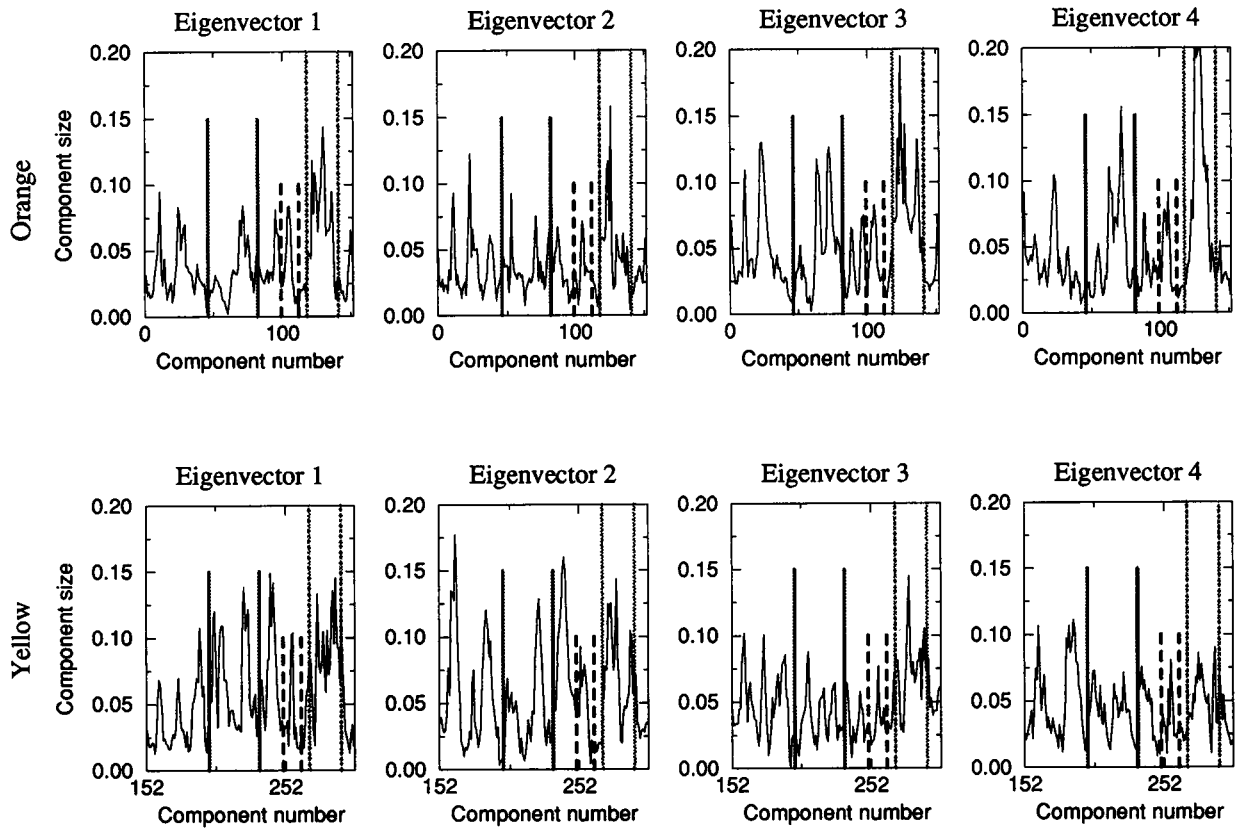

FIGURE 5 Absolute value of the components of the first four eigenvectors for each SOD subunit (absolute values). The four upper graphs represent the orange subunit, and the four lower graphs represent the yellow subunit. Boundaries of the loop regions: ——, loop 6, 5; – – –, loop 4, 7; ·····, loop 7, 8.

trajectory on selected eigenvectors are shown. The motion "period" of the first eigenvector is larger than the time range of the simulation. Eigenvectors 2, 3, and 4 show an almost "cyclic" motion. Starting from eigenvector 10, no relevant motion can be detected, and only Gaussian oscillations around an average value are observed.

Instantaneous asymmetrical motion of the two monomers

Fig. 5 indicates that the dynamic behavior of the two monomers is instantaneously asymmetrical, whereas in a protein made of two identical subunits, associated in a symmetrical way, we should expect that the atomic motions are invariant with respect to the symmetry of the dimer. This does not imply that at each time the molecule should be symmetrical, but that every type of motion and its "symmetric" (obtained by applying the symmetry operation, which exchanges the subunits) should have identical average properties. The symmetrical vector corresponding to each eigenvector may be obtained by applying the symmetry operation on the eigenvector and is not expected to be another eigenvector, because symmetrical vectors are not generally orthogonal in the configurational space. In this case, application of the symmetry operation to a given eigenvector generates a vector that can be expressed as a linear combination of the eigenvectors.

To check if the essential subspace has been significantly sampled, we have analyzed the motion along the vectors symmetrical to the eigenvectors.

In Fig. 7 we show the average square fluctuations along vectors symmetrical to the first 500 eigenvectors. From the figure it is evident that most of the fluctuation is confined to the first 100 vectors and that this curve is highly correlated with the curve of Fig. 4, which reports the eigenvectors against their relative eigenvalues. In particular, the first 10–15 symmetrical vectors have the highest fluctuation values, which implies that a simulation of ~300 ps produces a significant sampling of these directions. In particular, their values are comparable in size to the eigenvalues corresponding to the eigenvectors of indices in the range 5–10. In Fig. 8 we show the cumulative square projections of vectors 1–4, 50, and 250 symmetrical to the corresponding eigenvectors onto the first 500 eigenvectors. Vectors 1–4 are largely defined within the first 50 eigenvectors, whereas vectors 50 and 250 can reach a comparable cumulative square projection only within 150 and 250 eigenvectors, respectively.

These results imply that our simulation provides a reliable sampling of the phase space and gives a good indica-

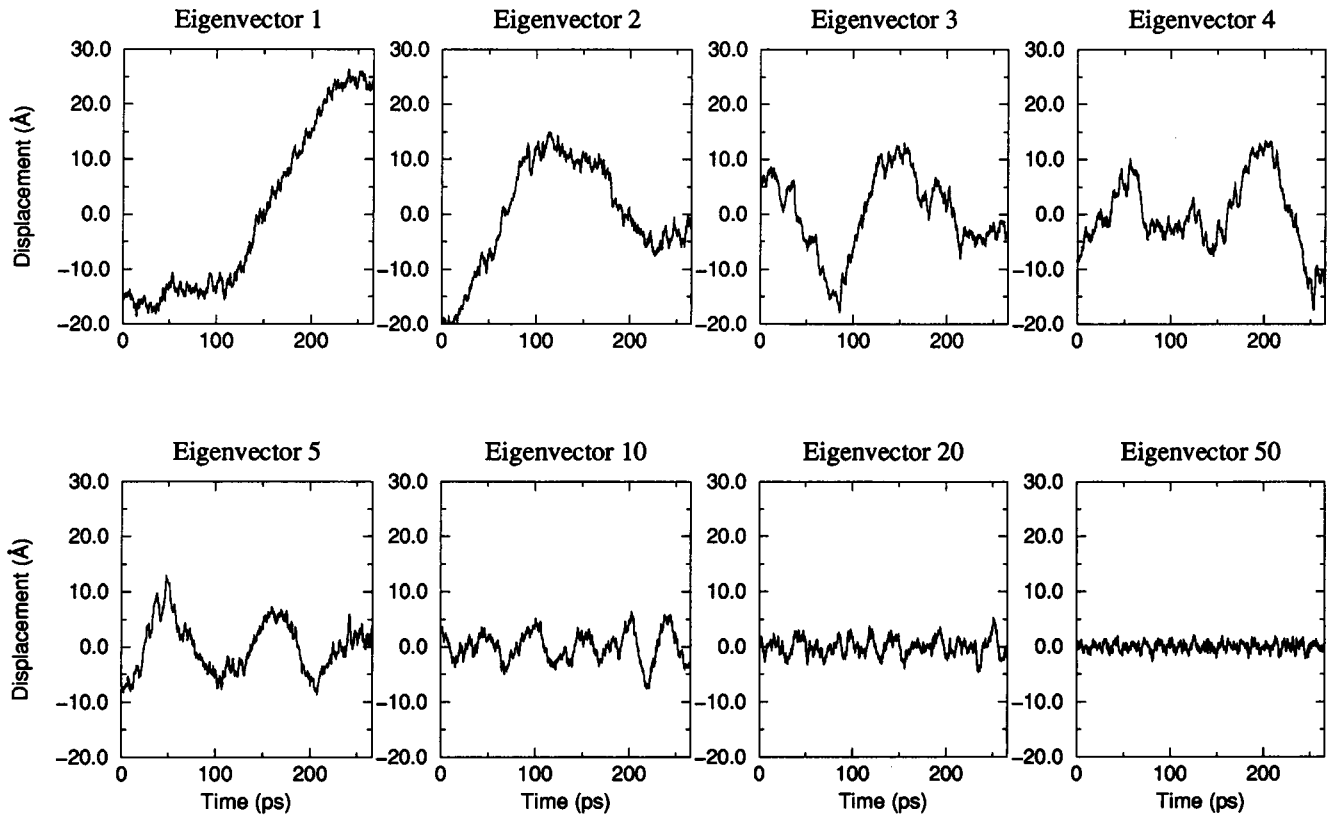

FIGURE 6 Projections of the simulation frames on selected eigenvectors.

tion that although the motion of the dimer is instantaneously asymmetrical it can be expected that on the average the motions of the two subunits will exchange.

Structural motions

To better localize the main regions involved in the protein motions, the components of the first four eigenvectors have been represented as individual 3D vectors originating from the C_α atoms of the time-averaged structure of the protein. This "C_α-arrows" representation is useful in understanding the localization of the protein motions for each eigenvector. It must be pointed out that the arrows indicate the direction of the motion, whereas the intensity and versus can change, only coherently and simultaneously, for all of the arrows.

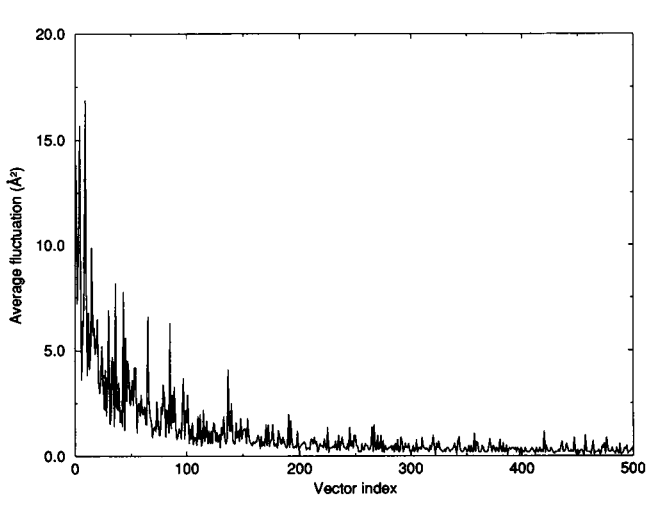

FIGURE 7 Amount of motion (average square fluctuation) along vectors symmetrical with respect to the eigenvectors.

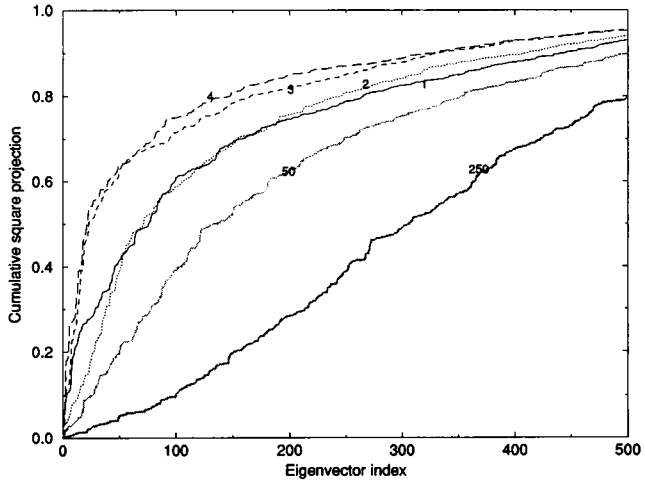

FIGURE 8 Cumulative square projections of the vectors symmetrical to the eigenvectors onto the first 500 eigenvectors. ——, vector 1; ·····, vector 2; – – –, vector 3; — —, vector 4; , vector 50; ——, vector 250).

The motions observed are mainly concentrated in two large regions of the protein subunit. The first, of higher intensity, involves the subdomains including the major loops of SOD (6, 5 and 7, 8); the second, of lower intensity, involves the subdomains forming the antiparallel β-barrel. The structural fluctuations corresponding to each eigenvector are generated by a different combination of the motions involving the loops and the β-barrel, and the resulting global motion of each eigenvector has an asymmetrical character.

The motions evidenced by the first eigenvector are reported in Fig. 9. These motions are mainly concentrated on the Zn-ligand region of loop 6,5 and the electrostatic loop 7,8, whereas the β-barrels are less mobile than the loops. The direction of the motion of loop 7,8 is different in the two subunits, pointing alternately toward the solvent and toward the protein in the Orange and Yellow subunits, respectively. The resulting motion in the two subunits is asymmetrical, in both direction and intensity, being of higher intensity in the Yellow compared to the Orange subunit (see also Fig. 5). Loop 4,7, which is the only loop connecting the two β-sheets in each monomer, simultaneously points toward or away from the dimer interface. In the protein orientation of Fig. 9, loop 4,7 is not clearly shown.

Analysis of this eigenvector indicates that the β-barrel acts as a framework into which loops 6,5 and 7,8 are inserted, and these are free to fluctuate, modifying the shape of the active site. In SOD at physiological conditions, the rate-limiting step of the catalytic reaction is the collision between the substrate and the catalytic site, which is known to be electrostatically controlled (Desideri et al., 1992; Sergi et al., 1994). The motion observed in this eigenvector produces a reorganization of the loops constituting the electrostatic channel to enhance the interaction with the substrate.

The motions corresponding to the second eigenvector are represented in Fig. 10 with the same protein orientation of the previous picture. The motion, as for the previous eigenvector, is of higher intensity in the Yellow (see also Fig. 5) than in the Orange subunit. In the Yellow subunit, the regular β-sheet of the β-barrel and the major loops 6,5 and 7,8 move coherently in opposite directions. At the same time, there is a small-intensity motion of the Orange subunit toward and away from the Yellow one (Fig. 10). Loop 4,7 is characterized by a motion similar to that described for the first eigenvector.

The C_α components of the third eigenvector are shown in Fig. 11. The orientation of the protein is different from that shown in Figs. 9 and 10. The motion may be divided into two circular movements of opposite direction, each involving one subunit. In this representation the β-barrel framework pushes toward loops 6,5 and 7,8 of the same subunit, twisting loop 4,7 downward, moving it toward the interface. The motions of higher intensity are localized in loops 6,5 and 7,8 of the Orange subunit (see Fig. 5). It must be pointed out that the direction of motion may be reversed.

The C_α components of the fourth eigenvector are represented on the dimer in Fig. 12 in the same orientation as in Figs. 9 and 10. The motions are mainly concentrated on loops 6,5 and 7,8 of the Orange subunit (see also Fig. 5). The direction of motion follows the external arrows represented in the figure. The Yellow 6,5 and 7,8 loops move, with low intensity, toward the β-barrel of the same subunit and then toward the dimer interface. The motion transmitted to the Orange β-barrel is finally released to external loops 6,5 and 7,8 of the same subunit, which move outward in the solvent. In this asymmetrical motion, the dynamic coupling between the two subunits is correlated with the large motions on the Orange loops, which result in a fluctuation of

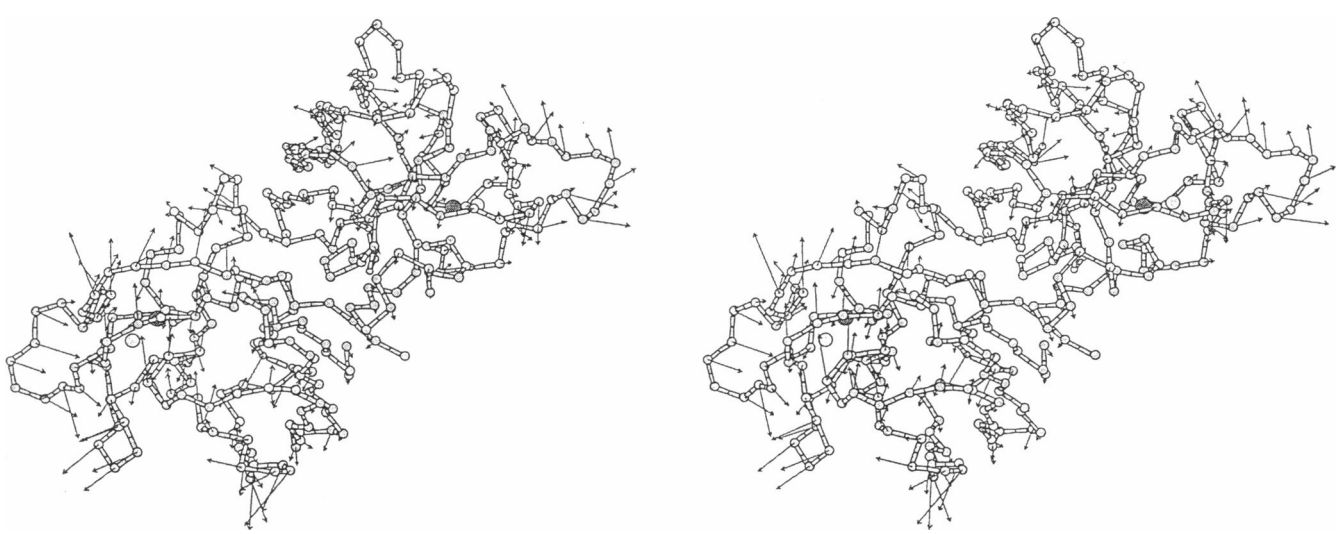

FIGURE 9 The motions of the first eigenvector are represented by arrows associated with each C_α atom on a ball-and-stick stereo representation of the SOD dimer. The copper ion is represented by a dark sphere, and the zinc ion is shown as a light gray sphere. The orange and the yellow monomers are represented in the upper right and in the lower left parts of the picture, respectively.

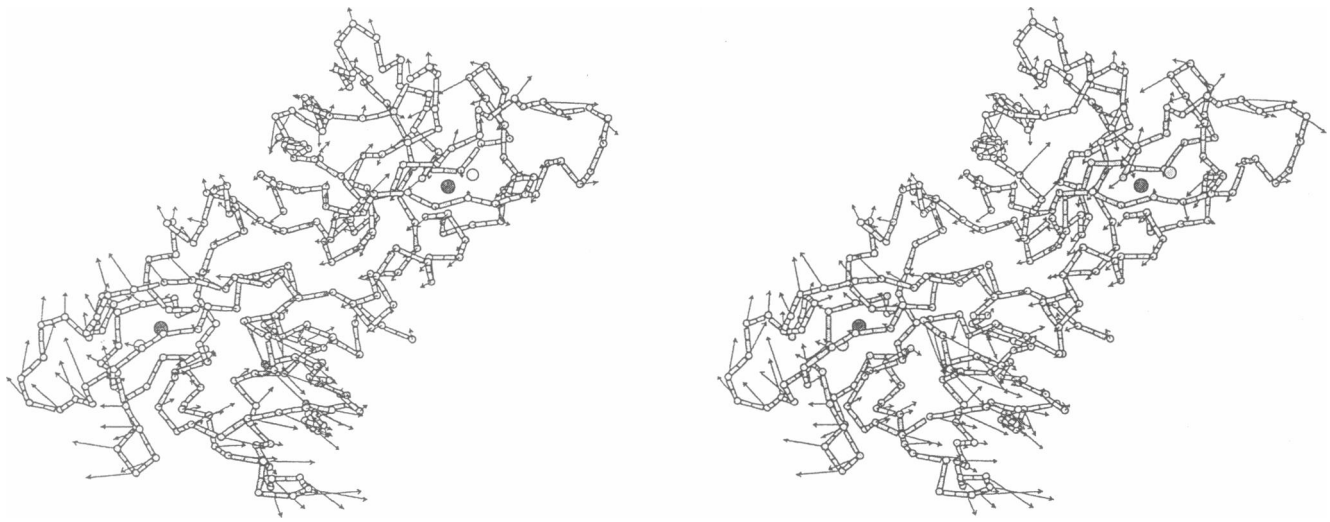

FIGURE 10 Same as Fig. 9, but for the second eigenvector.

residues located at the active site border, which must be flexible to facilitate the enzyme-substrate interaction.

Structural perturbation in the linear response limit

In the linear response limit, the covariance matrix can yeld insights into the structural response of the molecule when small perturbations are introduced. This can be obtained by the Green's function/principal component analysis (cf. Wong et al., 1993). If a set of small forces is applied to the atoms of the molecule, the change in the average atomic positions can be obtained from

$$\Delta\langle \mathbf{x} \rangle = \beta \tilde{C} \mathbf{F}^{\mathrm{p}} \tag{2}$$

where $\beta = 1/kT$ and $\mathbf{F}^{\mathrm{p}}$ are the perturbation forces, and $\tilde{C}$ represents the correlation matrix. From this equation it follows that when a force $F^{\mathrm{p}}_{\mathrm{ix}}$, such that $\beta F^{\mathrm{p}}_{\mathrm{ix}} = 1$, is applied to a single atom, i, in the x direction, its effect on atom j is

$$\begin{aligned} \Delta R^2_{\mathrm{jix}} &= \Delta\langle x_{\mathrm{j}} \rangle^2_{\mathrm{ix}} + \Delta\langle y_{\mathrm{j}} \rangle^2_{\mathrm{ix}} + \Delta\langle z_{\mathrm{j}} \rangle^2_{\mathrm{ix}} \\ &= \langle \Delta x_{\mathrm{i}} \Delta x_{\mathrm{j}} \rangle^2 + \langle \Delta x_{\mathrm{i}} \Delta y_{\mathrm{j}} \rangle^2 + \langle \Delta x_{\mathrm{i}} \Delta z_{\mathrm{j}} \rangle^2 \end{aligned} \tag{3}$$

A similar displacement of atom j occurs when the same force is applied on atom i along the y and z directions. To obtain a single value from $\Delta R^2_{\mathrm{jix}}$, $\Delta R^2_{\mathrm{jiy}}$, and $\Delta R^2_{\mathrm{jiz}}$, the following averaging procedure has been carried out:

$$\Delta R_{\mathrm{ji}} = \left(\frac{\Delta R^2_{\mathrm{jix}} + \Delta R^2_{\mathrm{jiy}} + \Delta R^2_{\mathrm{jiz}}}{3} \right)^{1/2} \tag{4}$$

In Fig. 13 we report the matrix $a_{\mathrm{ji}} = \Delta R_{\mathrm{ji}}$, normalized to the maximum a_{ji} value. The j and i index represents the C_α of the jth and ith residues, respectively. The grey and black pixels correspond to $0.2 \leq a_{\mathrm{ji}} \leq 0.6$ and $0.6 \leq a_{\mathrm{ji}} \leq 1.0$, respectively, whereas no pixel is recorded for $a_{\mathrm{ji}} \leq 0.2$.

In the matrix, the lower left (*II*) and upper right (*III*) panels show the intrasubunit correlations in the Orange and

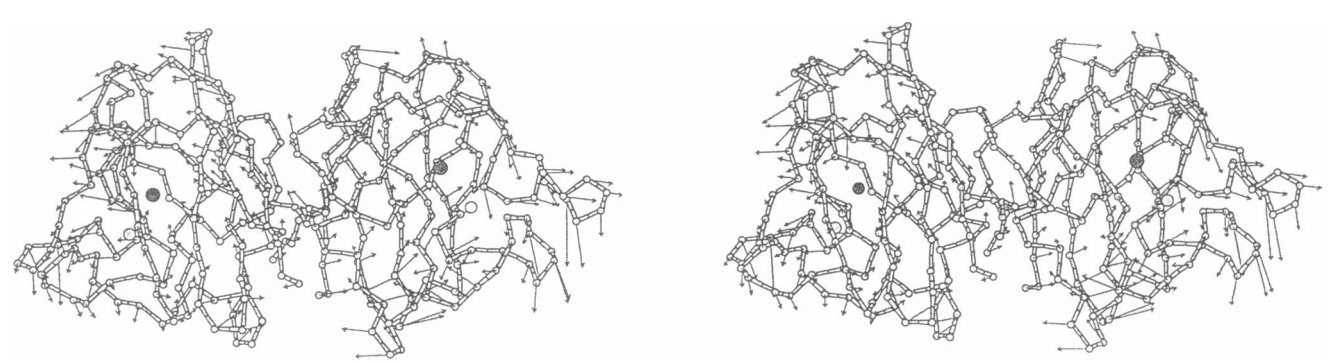

FIGURE 11 Same as Fig. 9, but for the third eigenvector. The protein is represented in a different orientation in which the orange and yellow monomers are displayed in the right and left parts of the picture, respectively.

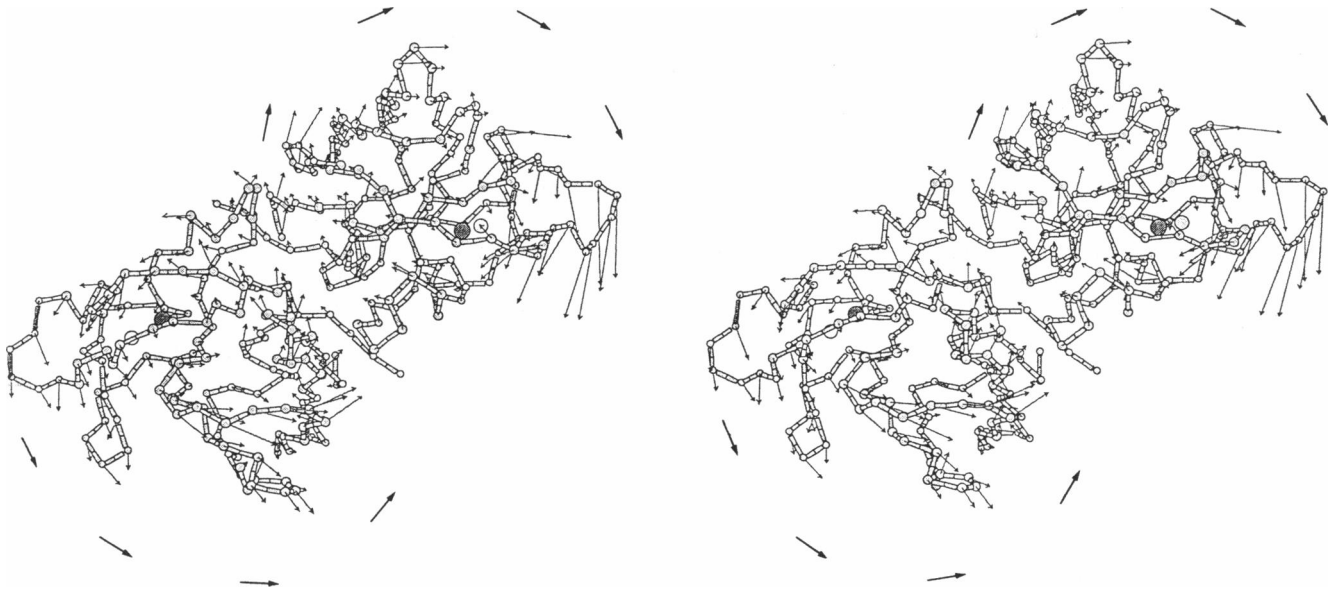

FIGURE 12 Same as Fig. 9, but for the fourth eigenvector. The external arrows indicate the direction of the motion observed in this eigenvector.

Yellow subunits, respectively. The two panels confirm that the motion in the two subunits is asymmetrical, inasmuch as the Yellow monomer shows an high degree of internal correlation if compared with the Orange subunit. It is interesting, however, that in both subunits the loop 7,8, which constitutes part of the electrostatic channel that modulates the collision of the substrate with the active site (Fisher et al., 1994; Polticelli et al., 1995), is entirely correlated with a large number of residue groups scattered along the protein sequence.

Interesting correlations are also observed between the two subunits (*I* and *IV*) where, in the same way, the electrostatic loop 7,8 and parts of the loops 4,7 and 6,5, including the region involved in the Zn binding, show correlations with several residues of the other subunit. These results confirm the data presented in the previous section and provide further evidence of the crucial role of loops 6,5 and 7,8, which are known to be involved in the substrate steering toward the catalytic copper atom (Sines et al., 1990; Polticelli et al., 1995; Fisher et al., 1994).

DISCUSSION

In the present paper we have reported the results of a 300-ps simulation of the dimer of SOD in solution. This is the longest simulation of the whole dimer in solution reported so far; however, it is still relatively short, and we are certainly far from full equilibration and sampling of the phase space accessible to the molecule. Nevertheless previously reported results (Amadei et al., 1993, 1996; van Aalten et al., 1995, 1996; Scheek et al., 1995; de Groot et al., 1996a,b,c) on proteins in solution have shown that the essential subspace of a protein can be reasonably determined by a simulation of a few hundred picoseconds. This is a crucial point in assessing the reliability of the present results. Analysis of the vectors symmetrical to the first eigenvectors supports the idea that the essential subspace has been significantly sampled. As the dimer is symmetrical, it is to be expected that on the average, an eigenvector and its symmetrical vector have the same amplitude. Figs. 7 and 8 show that essential subspace of symmetrical vectors corresponds to the essential subspace of eigenvectors; i.e., the first symmetrical vectors correspond to the first eigenvectors. We can conclude that, although a much longer simulation is required for an exhaustive sampling and statistics, the present simulation and analysis have likely detected the main features of the SOD dimer in solution.

The motions described in the four eigenvectors indicate that the two subunits behave at each instant in an asymmetrical way. This asymmetrical behavior is also evidenced by: 1) an r.m.s.d. different from that of the x-ray minimized structure (Fig. 3); 2) the different time exchange of the water molecule close to the copper site in the two subunits; 3) the projection of the motions on each C_α (Fig. 5); 4) the matrix shown in Fig. 13. It is important to notice that an independent MD study on the same protein (Falconi et al., 1996), carried out under different conditions, has also reported the occurrence of an asymmetrical dynamic for the two subunits.

Analysis of the second and the fourth eigenvectors suggests that concerted motions of large regions of one subunit (the loops and the β-barrel) influence the movement of the other subunit, leading to the hypothesis that the asymmetry between the two SOD monomers may be due to this intersubunit communication. The suggestion of an intersubunit communication also comes from the matrix of Fig. 13, which shows a correlation between several residues of one subunit and loop 7,8, loop 6,5, and loop 4,7 of the other

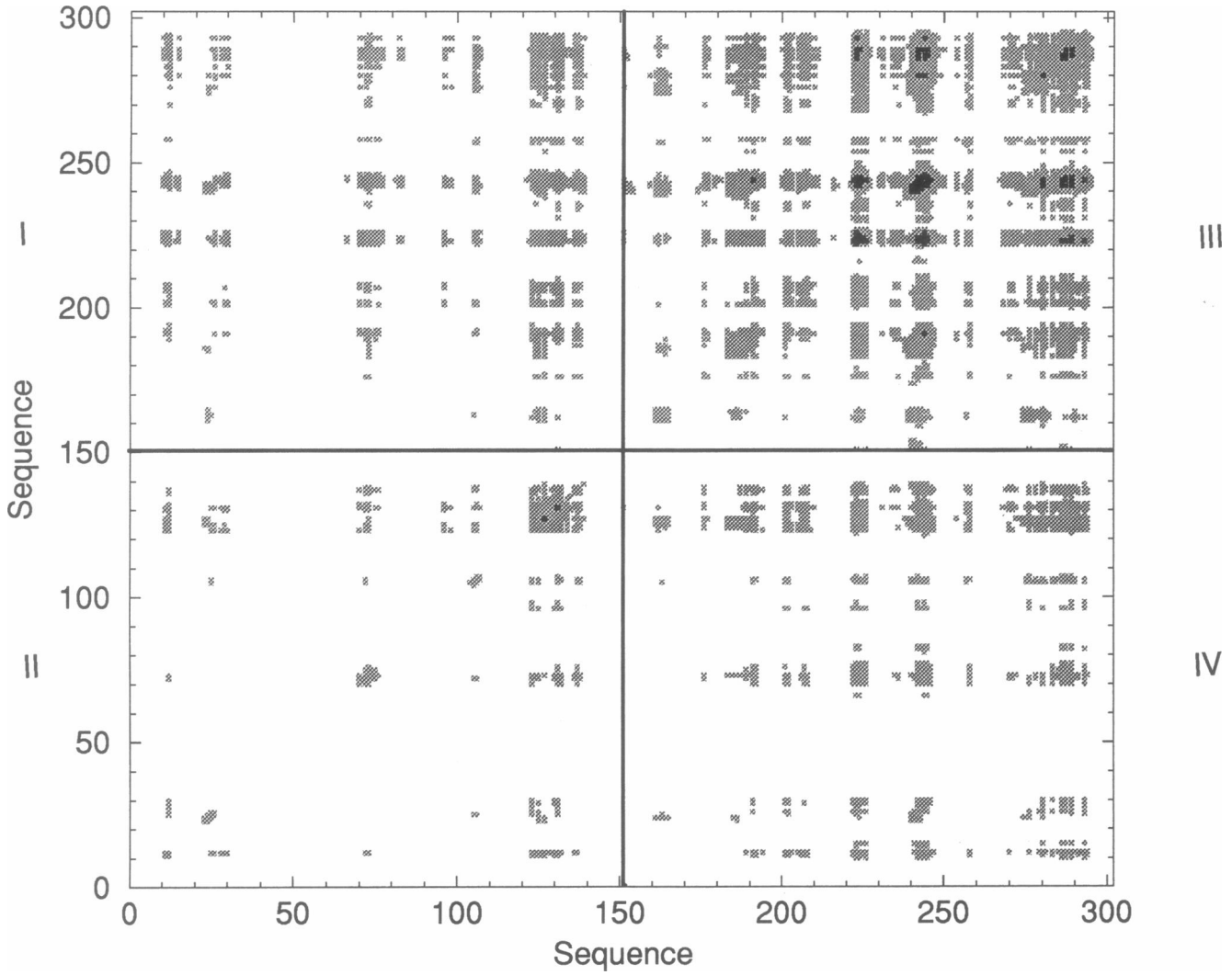

FIGURE 13 Displacement correlation matrix $\mathbf{a}_{ji}$ as defined in Eq. 4. The grey and black pixels correspond to $0.2 \leq \mathbf{a}_{ji} \leq 0.6$ and $0.6 \leq \mathbf{a}_{ji} \leq 1.0$, respectively, whereas no pixel is reported when $\mathbf{a}_{ji} \leq 0.2$. The upper-left square (*I*) and the lower-right square (*IV*) indicate the intersubunit correlations. The lower-left square (*II*) and the upper-right square (*III*) indicate the intrasubunit correlations in the orange and yellow subunits, respectively.

subunit. Loop 7,8 and loop 6,5 are the two major loops of SOD, which, together with the less regular β-sheet, accommodate the active site, and their motion is needed to organize the surrounding of the active site in a conformation that may allow the specific interaction of the catalytic copper with the superoxide. Previous MD studies (Shen et al., 1989; Shen and McCammon, 1991; Falconi et al., 1996) have indicated that the superoxide is directed toward the catalytic metal through the concomitant motions of several invariant residues located in the proximity of the active site. The significant role of protein fluctuations in the enzyme-substrate interactions has been confirmed by a study combining the use of Brownian and molecular dynamics in the presence of the substrate (Luty et al., 1993) and by MD calculations carried out on homology models of human Cu, Zn SOD mutants (Banci et al., 1992, 1994).

The simulation of the whole dimer in combination with the essential dynamics analysis allows us to highlight, in addition to the motion of the active site loops, the presence of correlated motions in the two subunits that suggest a mechanical coupling between the two subunits. This result is in agreement with the experimental evidence of a conformational communication between the two remote copper sites of the native dimer, detected as a break at one equivalent per mole of protein in either coulometric titration (Lawrence and Sawyer, 1979) or in the process of metal reconstitution of the apoprotein (Rigo et al., 1977, 1978).

Concerning the instantaneous asymmetrical behavior of the two subunits, it should be noted that from Figs. 7 and 8 we can conclude that our simulation provides a reliable sampling of the motion of the symmetrical vectors, suggesting that, over time, an exchange of the two subunits should occur. Our simulation cannot indicate the time needed to produce such an exchange, and work is in progress to lengthen the trajectory and estimate such a value. Because the second-order catalytic rate constant of this enzyme is

limited by the diffusion ($k_{cat}/K_M \approx 10^9\ M^{-1}\ s^{-1}$), determination of the time needed to exchange the motion of the two subunits would be of great importance to understanding whether the substrate meets a symmetrical or an asymmetrical enzyme, i.e., if both subunits work at the same time or in an alternate way. Up to now contradictory experimental results have been reported in the literature (Fielden et al., 1974; Cockle and Bray, 1977; Viglino et al., 1981).

The authors acknowledge the Ente Nazionale Energie Alternative group responsible for the benchmarking activity of the code within the Europort2/PACC project for making the simulation data available.

This work was partially supported by the Italian National Research Council special project "Sviluppo di algoritmi innovativi per la simulazione statica e dinamica." We thank CNR Italy for the financial support of G. Zimatore.

REFERENCES

Amadei, A., A. B. M. Linssen, and H. J. C. Berendsen. 1993. Essential dynamics of proteins. *Proteins Struct. Funct. Genet.* 17:412–425.

Amadei, A., A. B. M. Linssen, B. L. de Groot, D. M. F. van Aalten, and H. J. C. Berendsen. 1996. An efficient method for sampling the essential subspace of proteins. *J. Biomol. Struct. Dyn.* 13:615–625.

Andreani, C., A. Filabozzi, F. Menzinger, A. Desideri, A. Deriu, and D. Di Cola. 1995. Dynamics of hydrogen atoms in superoxide dismutase by quasi-elastic neutron scattering. *Biophys. J.* 68:2519–2523.

Banci, L., P. Carloni, G. La Penna, and P. L. Orioli. 1992. Molecular dynamics studies on superoxide dismutase and its mutants: the structural and functional role of Arg143. *J. Am. Chem. Soc.* 114:6994–7001.

Banci, L., P. Carloni, and P. L. Orioli. 1994. Molecular dynamics studies on mutants of Cu, Zn superoxide dismutase: the functional role of charged residues in the electrostatic loop VII. *Proteins Struct. Funct. Genet.* 18:216–230.

Bannister, J. V., W. M. Bannister, and G. Rotilio. 1987. Aspects of the structure, function and applications of superoxide dismutase. *CRC Crit. Rev. Biochem.* 22:111–180.

Berendsen, H. J. C., J. P. M. Postma, W. F. van Gunsteren, A. Di Nola, and J. R. Haak. 1984. Molecular dynamics with coupling to an external bath. *J. Chem. Phys.* 81:3684–3690.

Bernstein, F., T. Koetzle, G. Williams, E. Meyer, Jr., M. Brice, J. Rodgers, O. Kennard, T. Shimanouchi, and M. Tasumi. 1977. The protein data bank: a computer-based archival file for macromolecular structures. *J. Mol. Biol.* 112:535–542.

Cockle, S. A., and R. C. Bray. 1977. Do all the copper atoms in bovine superoxide dismutase function in catalysis? *In* Superoxide and Superoxide Dismutase. A. M. Michelson, J. M. McCord, and I. Fridovich, editors. Academic Press, London. 215.

Cupane, A., M. Leone, V. Militello, M. E. Stroppolo, F. Polticelli, and A. Desideri. 1994. Low-temperature optical spectroscopy of native and azide reacted bovine Cu, Zn superoxide dismutase. A structural dynamics study. *Biochemistry.* 33:15103–15109.

Cupane, A., M. Leone, V. Militello, M. E. Stroppolo, F. Polticelli, and A. Desideri. 1995. Low-temperature optical spectroscopy of cobalt in Cu, Co superoxide dismutase. A structural dynamics study of the solvent-unaccessible metal site. *Biochemistry.* 34:16313–16319.

de Groot, B. L., A. Amadei, and H. J. C. Berendsen. 1996a. Towards an exhaustive sampling of the configurational spaces of the two forms of the peptide hormone Guanylin. *J. Biomol. Struct. Dyn.* 13:741–751.

de Groot, B. L., A. Amadei, R. M. Scheek, N. A. J. van Nuland, and H. J. C. Berendsen. 1996b. An extended sampling of the configurational space of HPr of *E. coli*. *Proteins Struct. Funct. Genet.* 26:314–322.

de Groot, B. L., D. M. F. van Aalten, A. Amadei, and H. J. C. Berendsen. 1996c. The consistency of large concerted motions in proteins in molecular dynamics simulations. *Biophys. J.* 71:1707–1713.

Desideri, A., M. Falconi, F. Polticelli, M. Bolognesi, K. Djinovic, and G. Rotilio. 1992. Evolutionary conservativeness of electric field in the Cu, Zn superoxide dismutase active site. *J. Mol. Biol.* 223:337–342.

Djinovic, K., G. Gatti, A. Coda, L. Antolini, G. Pelosi, A. Desideri, M. Falconi, F. Marmocchi, G. Rotilio, and M. Bolognesi. 1992. Crystal structure of yeast Cu,Zn enzyme superoxide dismutase. Crystallographic refinement at 2.5 Å resolution. *J. Mol. Biol.* 225:791–890.

Djinovic-Carugo, K., A. Battistoni, M. T. Carrí, F. Polticelli, A. Desideri, G. Rotilio, A. Coda, and M. Bolognesi. 1994. Crystal structure of the cyanide-inhibited *Xenopus laevis* Cu, Zn superoxide dismutase at 98K. *FEBS Lett.* 349:93–98.

Djinovic-Carugo, K., A. Coda, A. Battistoni, M. T. Carrí, F. Polticelli, A. Desideri, G. Rotilio, K. S. Wilson, and M. Bolognesi. 1996. Three-dimensional structure of *Xenopus laevis* Cu, Zn superoxide dismutase B determined by x-ray crystallography at 1.5 Å resolution. *Acta Crystallogr.* D52:176–188.

Doster, W., S. Cusack, and W. Petri. 1989. Dynamical transition of myoglobin revealed by inelastic neutron scattering. *Nature.* 337: 754–756.

Falconi, M., R. Gallimbeni, and E. Paci. 1996. Dimer asymmetry in superoxide dismutase studied by molecular dynamics simulation. *J. Comput. Aided Mol. Des.* 10:490–498.

Fielden, E. M., P. B. Roberts, R. C. Bray, D. J. Lowe, G. N. Mautner, G. Rotilio, and L. Calabrese. 1974. The mechanism of action of superoxide dismutase from pulse radiolysis and electron paramagnetic resonance. Evidence that only half the active sites function in catalysis. *Biochem. J.* 139:49–60.

Fisher, C. L., D. E. Cabelli, J. A. Tainer, R. A. Hallewell, and E. D. Getzoff. 1994. The role of arginine 143 in the electrostatic and mechanism of Cu, Zn superoxide dismutase: computational and experimental evaluation by mutational analysis. *Proteins Struct. Funct. Genet.* 19: 24–34.

Gaber, B. P., R. D. Brown, S. H. Koening, and J. A. Fee. 1972. Nuclear magnetic relaxation dispersion in protein solutions. Bovine erythrocyte superoxide dismutase. *Biochim. Biophys. Acta.* 271:1–5.

Garcia, A. E. 1992. Large-amplitude nonlinear motions in proteins. *Phys. Rev. Lett.* 68:2696–2699.

Getzoff, E. D., D. E. Cabelli, C. L. Fisher, H. E. Parge, M. S. Viezzoli, L. Banci, and R. A. Hallewell. 1992. Faster superoxide dismutase mutants designed by enhancing electrostatic guidance. *Nature.* 358:347–351.

Getzoff, E. D., J. A. Tainer, P. K. Weiner, P. A. Kollman, J. S. Richardson, and D. C. Richardson. 1983. Electrostatic recognition between superoxide and copper zinc superoxide dismutase. *Nature.* 306:287–290.

Hayward, S., A. Kitao, F. Hirata, and N. Go. 1993. Effect of solvent on collective motions in globular proteins. *J. Mol. Biol.* 234:1207–1217.

Ichiye, T., and M. Karplus. 1991. Collective motions in proteins; a covariance analysis of atomic fluctuations in molecular dynamics and normal mode simulations. *Proteins.* 11:205–217.

Kabsch, W., and C. Sander. 1983. Dictionary of protein secondary structure: pattern recognition of hydrogen-bonded and geometrical features. *Biopolymers.* 22:2577–2637.

Klapper, I., R. Hagstrom, R. Fine, K. Sharp, and B. Honig. 1986. Focusing of electric fields in the active site of Cu-Zn superoxide dismutase: effects of ionic strength and amino-acid modification. *Proteins Struct. Funct. Genet.* 1:47–59.

Kraulis, P. J. 1991. MOLSCRIPT: a program to produce both detailed and schematic plots of protein structures. *J. Appl. Crystallogr.* 24:946–950.

Lawrence, G. D., and D. T. Sawyer. 1979. Potentiometric titrations and oxidation-reduction potentials of manganese and copper-zinc superoxide dismutases. *Biochemistry.* 18:3045–3050.

Luty, B. A., S. El Amrani, and J. A. McCammon. 1993. Simulation of the bimolecular reaction between superoxide and superoxide dismutase: synthesis of the encounter and reaction steps. *J. Am. Chem. Soc.* 115: 11874–11877.

Polticelli, F., A. Battistoni, P. O'Neill, G. Rotilio, and A. Desideri. 1996. Identification of the residues responsible for the alkaline inhibition of Cu,Zn superoxide dismutase: a site-directed mutagenesis approach. *Protein Sci.* 5:248–253.

Polticelli, F., G. Bottaro, A. Battistoni, M. T. Carrí, K. Djinovic-Carugo, M. Bolognesi, P. O'Neill, G. Rotilio, and A. Desideri. 1995. Modulation of the catalytic rate of Cu, Zn superoxide dismutase in single and double

mutants of conserved positively and negatively charged residues. *Biochemistry.* 34:6043–6049.

Rigo, A., P. Viglino, M. Bonori, D. Cocco, L. Calabrese, and G. Rotilio. 1978. The binding of copper ions to copper-free bovine superoxide dismutase. Kinetic aspects. *Biochem. J.* 169:277–280.

Rigo, A., P. Viglino, L. Calabrese, D. Cocco, and G. Rotilio. 1977. The binding of copper ions to copper-free bovine superoxide dismutase. Copper distribution in protein samples recombined with less than stoichiometric copper ion/protein ratios. *Biochem. J.* 161:27–30.

Romo, T. D., J. B. Clarage, D. C. Sorensen, and G. N. Phillips, Jr. 1995. Singular value decomposition analysis of time-averaged crystallographic refinement. *Proteins.* 22:311–321.

Ryckaert, J. P., G. Ciccotti, and H. J. C. Berendsen. 1977. Numerical integration of the cartesian equations of motions of a system with constraints: molecular dynamics of *N*-alkanes. *J. Comp. Phys.* 23: 327–341.

Scheek, R. M., N. A. J. Van Nuland, B. L. De Groot, A. B. M. Lissen, A. Amadei. 1995. Structure from NMR and molecular dynamics: distance restraining inhibits motion in the essential subspace. *J. Biomol. NMR.* 6:106–111.

Sergi, A., M. Ferrario, F. Polticelli, P. O'Neill, and A. Desideri. 1994. Simulation of superoxide-superoxide dismutase association rate for six natural variants. Comparison with the experimental catalytic rate. *J. Phys. Chem.* 98:10554–10557.

Shen, J., and J. A. McCammon. 1991. Molecular dynamics simulation of superoxide interacting with superoxide dismutase. *Chem. Phys.* 158: 191–198.

Shen, J., S. Subramaniam, C. F. Wong, and J. A. McCammon. 1989. Superoxide dismutase: fluctuations in the structure and solvation of the active site channel studied by molecular dynamics simulation. *Biopolymers.* 28:2085–2096.

Shen, J., C. F. Wong, S. Subramaniam, T. A. Albright, and J. A. McCammon. 1990. Partial electrostatic charges for the active center of Cu, Zn superoxide dismutase. *J. Comp. Chem.* 11:346–350.

Sines, J. J., S. A. Allison, and J. A. McCammon. 1990. Point charge distributions and electrostatic steering in enzyme/substrate encounter: Brownian dynamics of modified copper/zinc superoxide dismutases. *Biochemistry.* 29:9403–9412.

Sneddon, S. F., and C. L. Brooks, III. 1993. Protein motions: structural and functional aspects. *In* Molecular Structures in Biology. R. Diamod, T. F. Koetzle, K. Prout, and J. S. Richardson, editors. Oxford University Press, Oxford. 115–163.

Tainer, J. A., E. D. Getzoff, K. M. Beem, J. S. Richardson, and D. C. Richardson. 1982. Determination and analysis of 2 Å structure of copper zinc superoxide dismutase. *J. Mol. Biol.* 160:181–217.

van Aalten, D. M. F., A. Amadei, A. B. M. Linssen, V. G. H. Eijsink, G. Vriend, and H. J. C. Berendsen. 1995. The essential dynamics of thermolysin: confirmation of the hinge-bending motion and comparison of simulations in vacuum and water. *Proteins Struct. Funct. Genet.* 22:45–54.

van Aalten, D. M. F., B. L. de Groot, J. B. C. Findlay, H. J. C. Berendsen, and A. Amadei. 1996. A comparison of techniques for calculating protein essential dynamics. *J. Comput. Chem.* 18:169–181.

van Gunsteren, W. F., and H. J. C. Berendsen. 1987. GROMOS: Groningen Molecular Simulation (GROMOS) Library Manual. Biomos, Groningen.

Viglino, P., A. Rigo, E. Argese, L. Calabrese, D. Cocco, and G. Rotilio. 1981. ^{19}F relaxation as a probe of the oxidation state of Cu, Zn superoxide dismutase. Studies of the enzyme in steady-state turnover. *Biochem. Biophys. Res. Commun.* 100:125–130.

Vriend, G. 1990. WHAT IF. A molecular modeling drug design program. *J. Mol. Graph.* 8:52–56.

Wong, C. F., C. Zheng, J. Shen, A. McCammon, and P. G. Wolynes. 1993. Cytochrome *c*: a molecular proving ground for computer simulations. *J. Phys. Chem.* 97:3100–3110.

Wong, Y., T. W. Clark, J. Shen, and J. A. McCammon. 1993. Molecular dynamics simulation of substrate-enzyme interactions in the active site channel of superoxide dismutase. *Mol. Simul.* 10:277–289.